KOM
CORROSION AND MATERIAL PROTECTION JOURNAL
ORIGINAL ARTICLE
sciendo

Synergistic effect of acetic acid and NO_X for objects made of lead and its alloys; indoor corrosive environments in museums and depositories

Majtás D., Mácová P., Adámková I., Viani A.
Czech Academy of Sciences, Institute of Theoretical and Applied Mechanics, Prague, Czech Republic
E-mail: majtas@itam.cas.cz

Complex corrosion simulation to evaluate synergistic effect have to cover large number of factors. To do so, environmental and corrosion datasets collected by monitoring sites of interest have been used to tailor complex artificial ageing of lead and lead alloys, using lead, tin and tin-lead coupons. Material composition was based on objects of interest which are tin-lead alloy based although naming lead objects is used widespread for vast of them. To evaluate results corrosion rate based on weight loss, phase composition of corrosion product and colour change of the coupon surface were utilized. For thin corrosion layers formed micro Raman and FTIR did not provide suitable results, and GIXRD have been used.
Although limited number of conditions were used for the simulations, synergistic effect was observed for lead under specific conditions. Synergistic effect do occur on lead when exposed to NOX and acetic acid fumes of relatively low concentrations (18 µg·m-3 and 500 ppb respectively).

In addition, there is grouping of colourimetric data collected according to test regimes – phase composition of corrosion product respectively. This information albeit preliminary suggests that colourimetric spectroscopy may be suitable as fast and easy corrosion monitoring.

INTRODUCTION

The processes leading to metal corrosion and degradation are caused by different factors. Considering outdoor corrosivity, SO_2 and NO_X, are the main pollutants to be taken into account. Corrosivity at given location is driven by the concentration of pollutants and decreases according to distance from the source of pollution [1]. Improvements in technologies and new legislation from the ’70s of the last century, contributed to a decrease in concentration of pollutant in atmosphere and, consequently, led to a decrease in the corrosion rates [1,2,3]. Moreover, with the decline in the concentration of SO_2, the main pollutant is nowadays NO_X [1,3].

Outdoor environment influence to corrosivity of indoor environment is marginally only, since concentration of other pollutants present indoor is usually much higher and are of different type. Typically, they are volatile organic compounds, source of these are show-cases or storage cabinets e.g. [4,5].

Wooden cabinets are still widely used in exhibition areas and deposits. These cabinets are thus significant source of compounds such as formaldehyde, formic acid and acetic acid [6].

Corrosion is known to affect objects made of lead and its alloys, but also a wider range of objects both of historical and cultural value, such as pigments, paper, limestone etc. [7,8].

In fact, lead, a material, which is relatively inert respect to inorganic chemicals, is prone to deterioration if exposed to volatile organic chemicals, especially organic acids and their fumes. For this reason, the revision of ISO standard was published in 2020 [9].

Other studies about the indoor corrosion of lead, taking into account additional parameters, such as storing and corrosion history of objects, were conducted [10-15]. As a part of literature research process works concerning synergistic and possible synergistic effect had been examined. However, these articles and studies were mainly considering outside environments, which do not take into account indoor pollutants, or were considering modern materials for electronics and electro-technics [16-20].

Corrosion product analysis commonly employs methods including Raman spectroscopy, Fourier transform infrared spectroscopy (FTIR), X-ray diffraction [11,13,15,21-23]; often used together with microscopy – both optical and SEM.

However, combining the use of monitoring objects – coupons [9, 24], alongside with monitoring relative humidity and temperature using datalogger and concentration of pollutants using passive samplers, has been considered extremely informative [5, 25-27]. To assess corrosivity for lead and also its alloys, following combination of coupons was used: lead, tin and tin-lead soldering alloy. In such case, susceptibility of both

metals and their alloys could be compared at given conditions in the system using same logic of combined set of coupons as in the ISO standard [9] and further works [5,11,25-27].

Integrating the results of all these methods will enable the identification of synergistic effects and characterization of the complex corrosion processes of lead and lead alloys objects.

EXPERIMENTAL

The testing procedure consisted of two phases: in the first phase, model samples under different conditions have been prepared, in the second phase, they have been analysed. Conditions for artificial ageing processes were selected according to previous results collected in the course of the project [5,28-31]. Specific artificial corrosive environments where reproduced and monitored in a corrosion chamber CTS C+10/600-SG.

Sample preparation

All metallic coupons used in this study were shaped as plates 80 × 30 mm with thickness identical to the thickness of the rolled metal sheet from which they have been cut (thickness varying from 0.75 to 1.5 mm depending on coupon material). Names used to identify them are as follows: ***P*** coupons are of lead, ***PS*** coupons are tin-lead soldering alloy Pb60Sn40, and ***S*** coupons are of tin.

Pre-existing corrosion layers were removed by mechanical and chemical treatment according to standards [24], surface of coupons was degreased, and flattened. After the corrosion products removal, samples were mounted onto plastic stand – sample holder – to be inserted into the corrosion chamber. The way coupons are organised in the chamber using sample holder had been developed previously at SVUOM used since on coupons made of various metallic materials repeatedly.

Experimental conditions were based on previous work [29, 31], the test duration was changed according to presence of pollutants in the test chamber and thus more aggressive conditions to 31 days in the climatic chamber under other conditions being constant during the test duration, as written in previous article [31].

During each test run in a climatic chamber, a set of 5 coupons per selected material is used during one test period. Weight loss is calculated from four samples per test run at least (assuming one coupon is saved for further additional analysis, stored in defined and controlled conditions).

Samples are located in plastic holder that is not affecting samples. Samples are inserted into the holder to ensure both active sides of the sample are available for contact with the exposure environment. Thus masking of the reverse side of the sample is not necessary. This experimental setup provides minimal coverage of the active surface through contact with the sample holder. Approximately 60 ° sample inclination also prevents liquid to cover the surface of the samples permanently. The sample holder is equipped with holes in the bottom to ensure the liquid neither condensates nor stays inside the sample holder.

Artificial ageing

The first phase was focused on monitoring the factors that may cause corrosion including their combination. They had been chosen to determine whether or not there is a possibility of synergistic effects that may worsen the corrosion. Both susceptibilities of lead, tin and their alloy and physical-chemical parameters of contemporary environment, to which objects are exposed, have been taken into account in the test procedure preparation.

The second phase was focused on finding suitable analytical methods for classification of the corrosion process and its results. This utilises several approaches both in corrosion rate classification, phase composition and matching corrosion products – phase composition – to colour and its change.

The main goal was to determine under which conditions synergistic effect occurs. The additional result and the reason behind the colourimetric spectroscopy usage was to determine if there is possibility to correlate colour change to phase composition and conditions of the corrosion process. Such a method is an easy to use first line of defence method. The method that museum and exhibition staff could use on the daily basis to monitor the situation and detect possible corrosion effects.

The conditions simulated in the chamber are reported in Tab. 1. In summary, they were aimed at evaluating:

- Effect of temperature on samples in corrosive environment (test regimes A-C).
- Effect of concentration of single pollutant in the environment (test regimes B, D and E)
- Effect of pollutants combination – Synergistic effect (test regime F)

Tab. 1. Summary of test regimes selected for artificial ageing

Test regime	T [°C]	RH [%]	c(CH_3COOH) [ppb]	c(NO_X) [µg.m^{-3}]
A	15	75	500	0
B	25	75	500	0
C	35	75	500	0
D	25	75	50	0
E	25	75	0	18
F	25	75	500	18

The value of CH_3COOH concentration used in accelerated laboratory tests is based on capabilities of wood and chipboard materials to evaporate volatile organic acids to indoor environment, as described in [5,6,9,26-28].

The value of NO_2 concentration 18 $\mu g \cdot m^{-3}$ used in accelerated laboratory tests of synergistic action of volatile organic acids, is based on the average concentration of this pollution in atmospheres in the Czech Republic and on statistical results of long-term measurements in outdoor and indoor atmospheres [1,3,15,30]. Higher concentrations of NO_2 can be expected even near local roads in municipalities and cities with intensive traffic, higher development and a dense local transport network (32 - 40 $\mu g \cdot m^{-3}$). The lowest NO_2 concentrations are frequently encountered at regional monitoring stations far from the emission sources. The typical indoor and outdoor pollution ratio (I/O) for nitrogen dioxide is in the range of 0.60 to 0.80, and so NO_2 concentrations in indoor environments near traffic roads can be assumed to be in the range of 19 to 32 $\mu g \cdot m^{-3}$ [3, 28].

Analytical methods

After preliminary evaluation of the sample surface by naked eye, spectrophotometry was employed to detect the colour coordinates of the coupons surface. An Avantes StarLine AvaSpec-2048 spectrophotometer (light source D65, 10° standard observer), with AvaSoft 8.0 processing software, was employed. For each sample, a total of six points were measured and values averaged. Data collected in reflection mode, were expressed in the colour space coordinates (in CIE Lab, CIE Lhc, CIE XYZ). Details on the method, developed during previous work in the scope of the project, are available in article [31].

Further quantitative evaluation was carried out by calculating the corrosion rate from weight loss of the sample using sequential pickling as described in the standard ISO [24]. Coupons were used at the scope and interval pickling was chosen according to the ISO standard [24]. Pickling agent used for the pre-treatment was hydrochloric acid. Conditions for pickling for tin, and tin-lead alloy are those named in the ISO standard [24], for lead coupons conditions used for treatment are based on previous work in the scope of this project as mentioned in articles [5,29].

Phase composition of the corrosion products was determined with X-ray diffraction method, adopting a grazing incident geometry (GIXRD). At the scope, the coupons were placed on a movable XYZ stage of a Bragg-Brentano diffractometer Bruker D8 Advance (Bruker, Germany). Diffracted intensity was collected on a silicon strip detector by scanning in 2θ with the incident X-ray beam, produced with Cu K_α radiation, fixed at the angle $\theta = 0.5°$. This approach was deemed necessary since previous tests aimed at the identification of corrosion products adopting spectroscopic methods (micro-Raman and FTIR), were unsuccessful due to the reduced thickness of the corrosion layer [32]. The GIXRD spectra suffer from effects of preferred orientation of crystals and limited statistics, therefore, the results cannot be considered fully quantitative although suitable for phase identification.

RESULTS

Colour changes

The results of colourimetric tests evidenced differences between the samples with the conditions F for Sn coupons falling apart from the others.

Using CIE Lab colourspace more suitable are ***a*** and ***b*** colour coordinates then ***L*** coordinate. This is caused by the fact that the lightness coordinate does also include information on reflectance of the surface.

Graphical representation of collected data is reported in Figures 1-3, per each material type summarizing all test regimes for each material.

Perceptual lightness and thus reflectivity of lead and tin-lead soldering alloy coupons is more affected then colour change as shown in Fig. 1 and 2. This also indicates corrosion product is not homogeneous. For tin coupons, this is a bit different. For types shown on Fig. 3 in NO_X atmosphere, the corrosion product is not homogeneous in colour significantly, but in case of synergistic environment the results are more homogeneous.

There is no distinctive trend in colour change (comparing different temperatures of artificial ageing or concentrations of pollutants), however distinctive colour groups are formed according to test regime (which correlates with different phase composition). This observation will be discussed later.

Corrosion rates

Summarized results of average values of corrosion rates are shown in Tab. 2. Lead evidenced a high susceptibility to the effect of temperature, with the rate increasing more than three times from 15 to 35 °C. This susceptibility is also driving the trend observed in the PbSn alloy, since the pure Sn coupons did not show appreciable temperature dependence.

There is a difference as expected, when concentration of CH_3COOH increased (regimes D and B), corrosion rates for NO_x presence (regime E) are comparable with higher concentration of CH_3COOH (regime B) for tin and tin-lead solder alloy, however is significantly lower for lead (comparing regimes E and B).

To describe the effect of the combined presence of both pollutants (regime F), compared to single pollutant regimes: A, B, C and D where CH_3COOH is introduced,

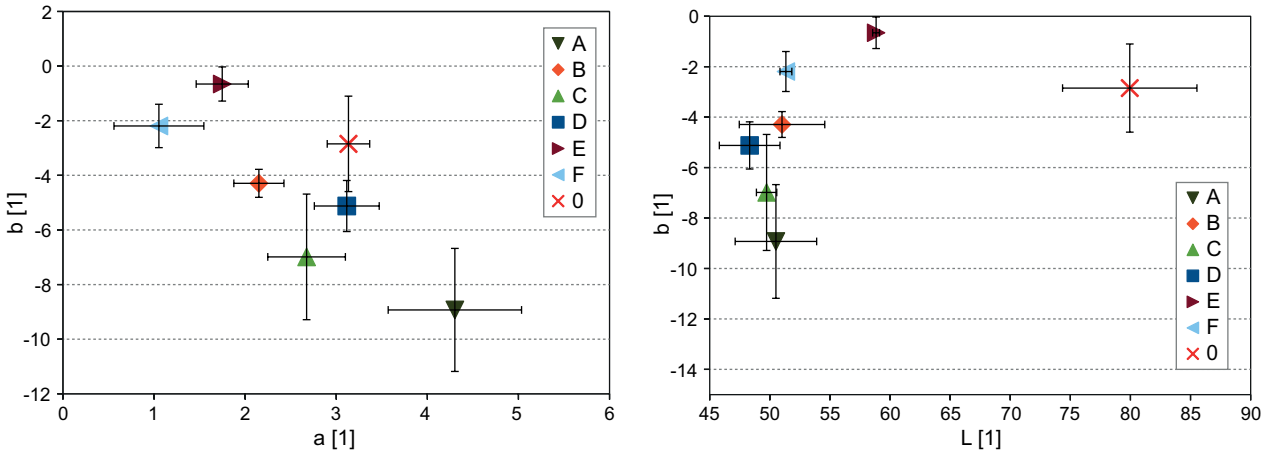

a) PbSn40 coupons (CIE LAB – ab) b) PbSn40 coupons (CIE LAB – Lb)

Fig. 1. CIE ab and CIE Lb data collected after test regimes from lead coupons – summary

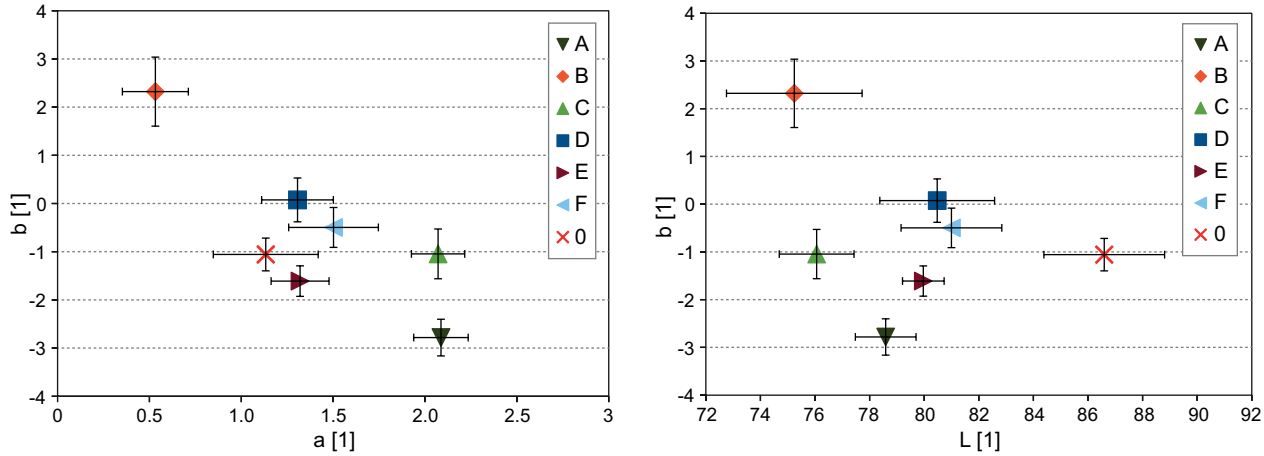

a) PbSn40 coupons (CIE LAB – ab) b) PbSn40 coupons (CIE LAB – Lb)

Fig. 2. CIE ab and CIE Lb data collected after test regimes from tin-lead soldering alloy coupons – summary

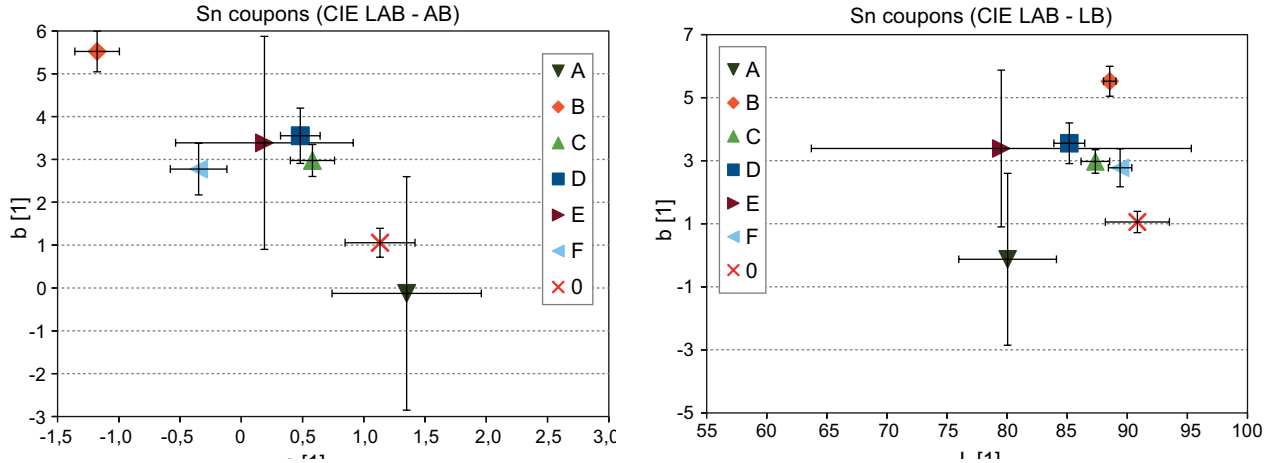

a) PbSn40 coupons (CIE LAB – ab) b) PbSn40 coupons (CIE LAB – Lb)

Fig. 3. CIE ab and CIE Lb data collected after test regimes from tin coupons – summary

and E, where NO_x is introduced, are considered. In both cases, an amplifying effect was obtained on the lead coupons, whereas a slight inhibiting effect was observed for the other coupons.

Due to the test duration (31 days) and previous published in works [28, 29], corrosion rate under given conditions for given sets of coupons could be calculated in form of weight loss per square meter during a period of 1 year. Initiating period of corrosion process where the process is in unstable state when corrosion layers are forming faster than the rest of the further corrosion product evolution where its time evolution is linear and process of corrosion is in stable state as described in [28].

However, one have to keep in mind that there are limitations for weight change depending on coupon geometry and material. Figures 4-6 show comparison of weight loss during pickling process (normalized values using fraction of starting coupon weight).

In the environment with lower corrosivity affecting the coupon, lower weight loss is observed. Such situation could be demonstrated on tin coupons from test regime B – Fig. 6, where weight change between pickling steps is comparable to accuracy of used laboratory scales.

The tin coupons on Fig. 6 still provide some information, as there is still trend visible in the dataset. But for environments with lower corrosivity either larger and thus heavier coupons or laboratory scales of higher accuracy would be needed.

Pickling behaviour of coupons from test regime C is a bit confusing. All presented data in the Fig. 5 were obtained from coupons from the exact same test run, thus effect of test regime malfunction that went unnoticed could be omitted. There was no visible difference on the sample both prior and after the pickling process (except slight colour differences of the corrosion products that are normal).Difference of gradient (derivative) for coupon

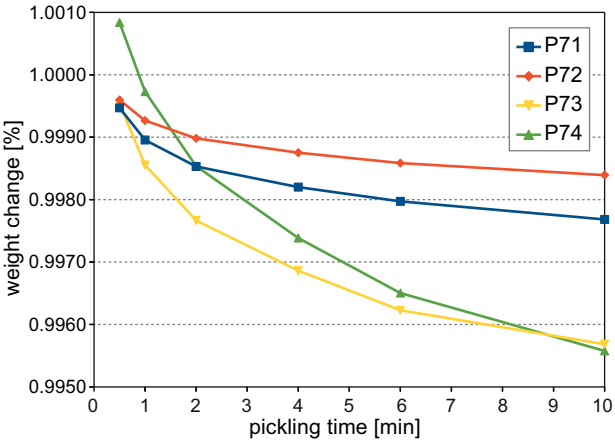

Fig. 5. Interval pickling of Lead coupons – test regime C

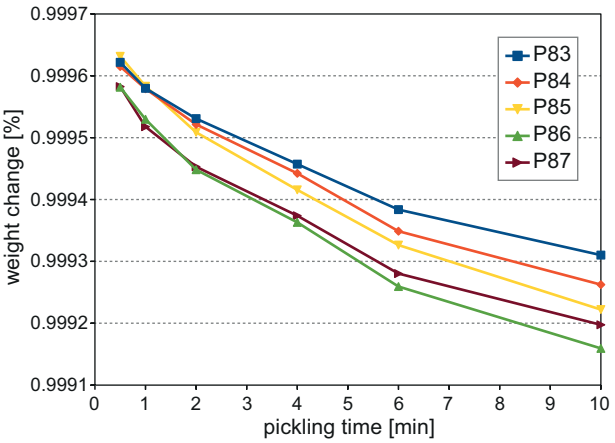

Fig. 4. Interval pickling of Lead coupons – test regime A

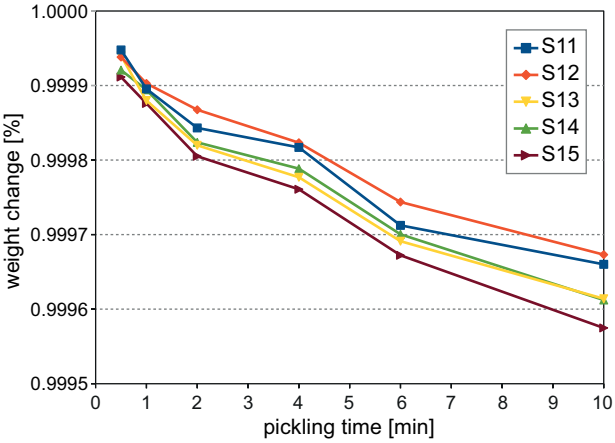

Fig. 6. Interval pickling of tin coupons – test regime B

Tab. 2. List of components in exposure cells

Test regime	v_{cor} (Pb) [g·m^{-2}·a^{-1}]	σ (Pb)	v_{cor} (PbSn) [g·m^{-2}·a^{-1}]	σ (PbSn)	v_{cor} (Sn) [g·m^{-2}·a^{-1}]	σ (Sn)
A	32.0611	1.9758	3.8703	0.5071	4.3359	0.4054
B	64.8045	3.7008	4.4994	0.8651	3.1715	0.3673
C	108.9381	24.9851	5.6707	0.2426	4.3229	0.3251
D	44.9175	3.0276	3.8115	0.4214	3.7106	0.6202
E	14.3710	3.7008	4.7682	0.5487	3.3269	0.3673
F	115.4075	21.7820	3.9414	0.3149	4.2499	0.2778

P73 and especially for P74 may indicate not all corrosion products were removed, despite no observable difference in surface colouring or structure as noted above. In that particular situation P73 slope albeit visibly different from P71 and P72 is still in agreement with other results. Thus P74 should be omitted.

Conclusion or starting point for further research: replicate test regimes with given conditions for several times using longer pickling interval (total pickling duration) to ensure all corrosion products are removed even though in previous work in the scope of the project [5,28-31] nothing suggest presence of anomaly.

Phase analysis

Results from GIXRD are illustrated in Fig. 7. For corrosion products of lead in conditions F, the corrosion layer was thick enough to allow for collecting XRD data with a conventional θ-2θ scan.

Phase analysis results are shown in Tab. 3. For the test regimes A-C, a change in phase composition from $Pb_3(CO_3)_2(OH)_2$ to $Pb_5(CO_3)_3O(OH)_2$ was observed. It can be conjectured that this is related to the temperature increase. In fact, temperature dependence of formed corrosion products have been already observed [28], with different products of corrosion starting form lead acetate formed according to conditions in the test chamber.

Notably, in the regime D, corresponding to the lower amount of CH_3COOH, a mix of lead oxides was produced.

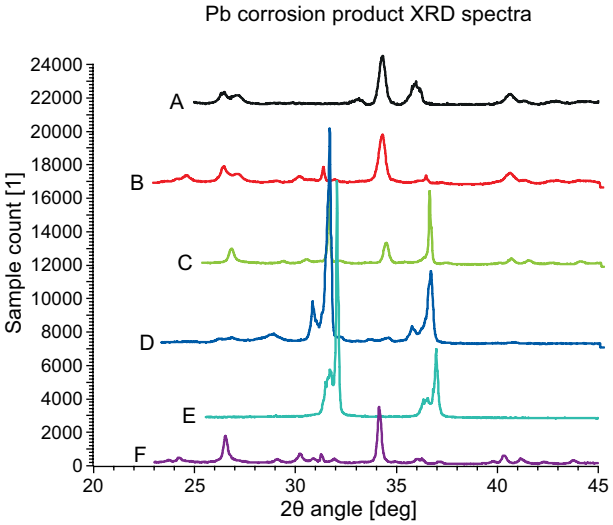

Fig. 7. XRD spectra obtained from GIXRD scan – summary (scan of regime F is θ-2θ scan)

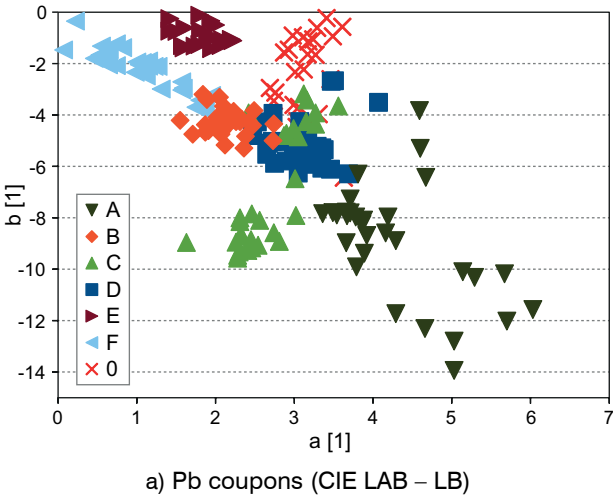

a) Pb coupons (CIE LAB – LB)

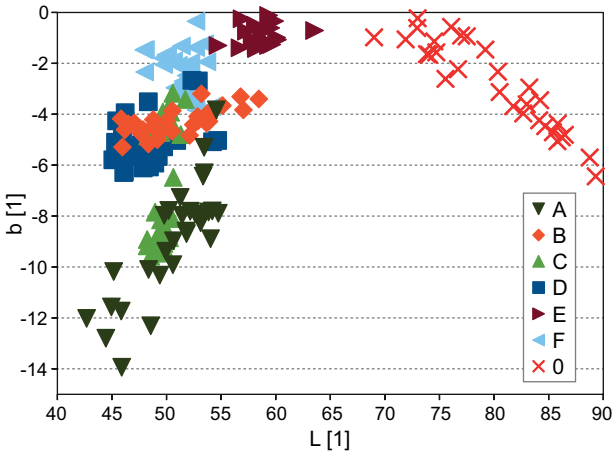

b) Pb coupons (CIE LAB – LB)

Fig. 8. CIE ab and CIE Lb data collected after test regimes from lead coupons – complete sets

Tab. 3. Phase composition of corrosion product analysed using GIXRD

Test regime	Pb	PbO	PbO_2	Pb_3O_4	$Pb_3(CO_3)_2(OH)_2$	$Pb_5(CO_3)_3O(OH)_2$
A	×				×	
B	×				×	×
C	×					×
D	×	×	×	×		
E	×					
F	×					×

In the coupons exposed to the combination of the two pollutants, only $Pb_5(CO_3)_3O(OH)_2$ was detected. Phase composition of these coupons was same as those of regime C, however main difference here is the amount of corrosion product formed during artificial ageing as could be seen from weight loss of coupons.

Absence of detectable phases of corrosion products for test regime E is caused by the small amount of corrosion product formed during the artificial ageing as can be seen from weight loss of coupons and by examination of coupons after the test by naked eye (compared to untreated coupons). Coupons of regime E should be further analysed using additional methods such as SEM-EDS to check for nitrogen containing corrosion products. The further analysis of these coupons is on schedule but have not been finished in the time of article preparation. This also applies for coupons from regime F (synergistic).

Results of colour measurement suggest that there is a corrosion product formed, but the layer thickness is too thin for GIXRG scan, and thus the corrosion product phase composition was not detected (or been masked by strong signal of Pb).

When the colourimetric data are considered, it can be noted that the gradual transition in the phase composition with the increase in temperature of the regimes A, B and C, is correlated with the distinct clustering of the corresponding values in the plot of **a** vs. **b** coordinates of the CIE LAB colour space (Fig. 8).

On the other hand, group of points corresponding to regime C are in overlap with those of regime D, although their phase composition is very different.

DISCUSSION

From the plots of CIE Lab colour coordinates of lead coupons, it can be observed that the data did not form discrete groups per artificial ageing regime. A way to improve their separation in order to provide a tool for the identification of the different regime is to use statistical analysis of dataset. This will reflect a correlation between colour information and phase composition of corrosion product. The result of discriminant analysis is shown in Tab. 4. Least accurate analysis is for the group C. This is in agreement with the data distribution of group C shown on Fig. 8.

There is difference between regimes A, B and C which is in agreement with the phase composition, although colour information obtained do not form linear behaviour as corrosion rates does for regimes A, B and C.

A dataset from regime A has wider spread that indicates corrosion product is not homogeneous. Dataset from regime C is forming two groups of which one do overlap with those of regime D. It further indicates additional phase analysis from different locations would be needed for such conditions. On the other hand, test

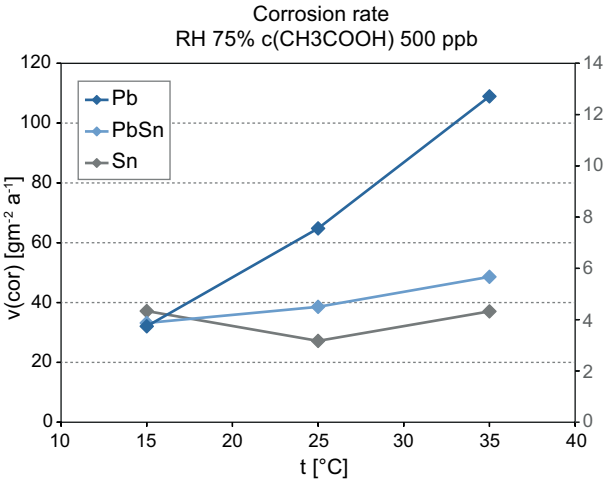

Fig. 9. Temperature dependence – summary (PbSn and Sn coupons use secondary Y axis – on the right side) at 75% relative humidity and 500 ppb acetic acid concentration

Tab. 4. Discriminant analysis of the Pb coupons colourimetric data, grouped by test regimes

	True Group						
Put into Group	**A**	**B**	**C**	**D**	**E**	**F**	**Untreated**
A	29	0	0	0	0	0	0
B	0	27	1	2	0	4	0
C	1	0	19	2	0	0	0
D	0	1	10	26	0	0	0
E	0	2	0	0	24	0	0
F	0	0	0	0	0	25	0
Untreated	0	0	0	0	0	0	30
Total N	30	30	30	30	24	29	30
N correct	29	27	19	26	24	25	30
Proportion	0.967	0.900	0.633	0.867	1.000	0.862	1.000

regimes D, E, F and B provides ddistinctive datasets. This could be also told about test regime A even though the data are spread on larger space and are not forming visibly coherent group.

Further phase analysis is needed to investigate heterogeneities in colour datasets. Collected phase composition data still suggest that there is correlation between colour information and phase composition.

The results of the test regimes A, B and C describe temperature dependence of corrosion rate. An increase in corrosion rate of lead and tin-lead alloy coupons could be observed. Lead is more affected by temperature change in the studied interval than tin-lead soldering alloy. This is in agreement with lead susceptibility to volatile organic acid fumes. Results are shown in Fig. 9.

Fig. 10 describes a dependence of corrosion rate on concentration of acetic acid. Corrosion rate of lead, tin-lead and tin coupon increases when the concentration of pollutant increases. Results of test regimes D and B are similar.

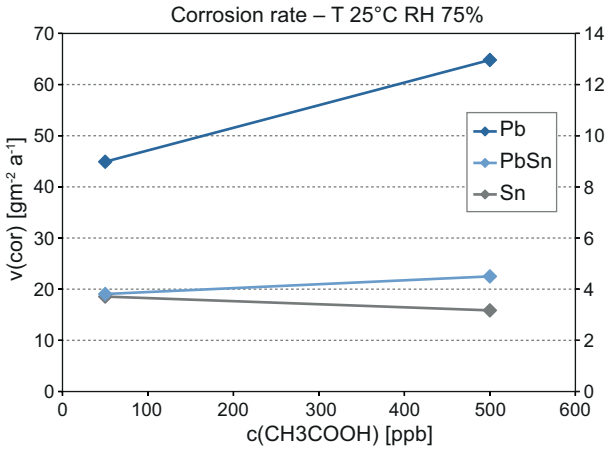

Fig. 10. CH_3COOH concentration dependence – summary (PbSn and Sn coupons use secondary Y axis – on the right side) at 75% relative humidity and 25 °C

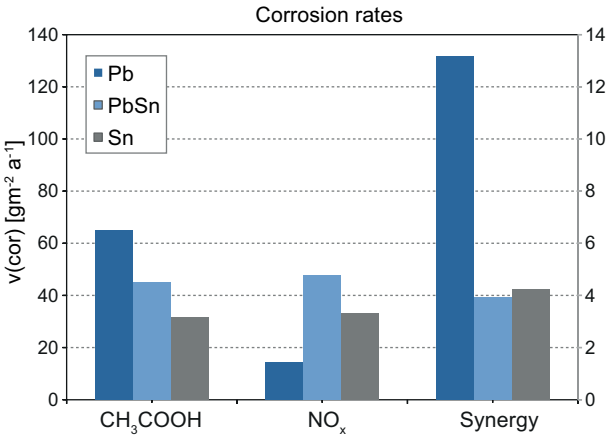

Fig. 11. Synergistic effect of pollutants on corrosion rate – summary (PbSn and Sn coupons use secondary Y axis – on the right side)

It is possible that corrosive conditions are not aggressive enough for Sn coupons at low temperatures and pollutant concentration, or the fact the lab scales used in combination of the size and thus weight of coupons used are not suitable (as noted previously).

Fig. 11 describes synergistic effect of concentrations of pollutants. Combining dependence of concentration change of CH_3COOH and NO_X, the results of the test regime F with both pollutants and the test regime C are similar, but previously noted XRD analysis without need of GIXRD is sign that there is some synergy occurring.

Comparing the corrosion rate of lead and tin-lead alloy, temperature is rather less crucial condition for cultural heritage objects according to phase composition, as the lead objects of cultural heritage are mainly lead alloys with some amount of tin (or tin objects with added amount of lead to prevent the tin pest). Those objects are thus less prone to degradation based only on temperature change.

CONCLUSIONS

Phase composition of corrosion products dependents on corrosivity. Corrosion rate increases with temperature. Dependence on temperature is indirect as the humidity condensation in given environment depends on the temperature (via dew point). Results obtained from test under various temperatures (regimes A, B and C) do not show any non-standard or unexpected behaviour (10 degrees temperature increment doubles the corrosion rate – literally). Corrosion rate also increases with increasing concentration of acetic acid (regimes D and B).

Combination of pollutants accelerate corrosion rate, especially in case of lead coupons. Corrosion rate of lead is significant under those conditions. In case of tin coupons, corrosion rate increase is not so pronounced (compared to lead coupons), albeit still observable. However, corrosion rate decreases for tin-lead coupons.

The GIXRD method is suitable for thin layer corrosion products analysis. It is possible to analyse corrosion products of lead using GIXRD method as shown on presented results. However, it should be noted that GIXRD is qualitative analytical method only, and no quantitative analysis could be made of its results.

It was not possible to obtain reliable results using FTIR and micro Raman when using coupons from test regimes (A-F). Thus for combination of coupon materials and test regime conditions used in this study, both the methods are not suitable for phase analysis. The reason behind this is that both the methods need a minimal thickness of examined layer and both the methods resulted in analysing material beneath those layers of interest. This however does not disapprove usage of FTIR or micro Raman in other studies.

Using standard XRD measurement setup instead of GIXRD was possible for lead coupons from regime F. This information supports the results of interval pickling of lead coupons from this test regime. Corrosion rate of tin increases slightly (compared to lead), thus conditions of regime F are more aggressive for tin, too.

On the contrary, corrosion rate of tin-lead (PbSn40 alloy) decreases. According to obtained corrosion rate results, the effect of combined CH_3COOH and NO_X atmosphere may provide some limited protection for tin-lead alloys. However, to approve this statement, further study is needed.

It should be also noted that the results presented here cover phase composition and approval of synergistic behaviour for lead (under conditions examined). To determine dynamics and kinetics of the system further study is needed.

Acknowledgement:

The authors gratefully acknowledge the support from the Ministry of Culture, CZ, in the framework of the NAKI II Project, No. DG18P02OVV050.

REFERENCES

1. Kreislová K. et al. *Corrosion maps of Czech Republic*, electronic database http://www.korozni-mapy.cz.
2. Knotková D., Kreislová K., Dean S.W. Jr. (Eds) *Isocorrag International Atmospheric Exposure Program: Summary Of Results*, ASTM Data Series 71, Stock No.: DS71, ISBN: 978-0-8031-7011-7.
3. Kreislova K. et al. Indoor Corrosivity in Klementinum Baroque Library Hall, Prague, *WIT Transactions on The Built Environment*, **2021**, 203, PI-123–PI-131.
4. Fuente D. et al. The effects of organic pollutants on metals in museums: corrosion products, synergistic effects and the influence of climatic parameter, In: *METAL 2013,* 16-20 September 2013, Edinburgh, Scotland. Interim Meeting of the ICOM-CC Metal Working Group, **2013**, 229–233.
5. Kreislova K. et al. Indoor corrosivity classification based on lead coupons, *KOM – Corrosion and Material Protection Journal*, 65 (4), **2021**, 7–12.
6. Saheb M., Dubus M. Indoor corrosivity in museums and archives assessment: standards and recommendations, In: *Proceedings of 7th Indoor Air Quality meeting*, 15-17 November 2006, Braunschweig, Germany, **2006.**
7. Valach J. et al. Public perception and optical characterization of degraded historic stone and mortar surfaces. In: *Proceedings of the International Conference on Heritage, Weathering and Conservation*, HWC-2006, 21-24 June 2006, Madrid, Spain. Case studies. London: Taylor&Francis Group, **2006**, 827–832.
8. Sarici D. E. Thermal deterioration of marbles: Gloss, color changes, *Construction and Building Materials*, **2015**, 102, 416–421.
9. ISO 11844:2020 Corrosion of metals and alloys – Classification of low corrosivity of indoor atmospheres, **2020.**
10. Angelini E., Grassini S. Underwater corrosion of metallic heritage artefacts, *Corrosion and conservation of cultural heritage metallic artefacts*, **2013**, 236–259.
11. Angelini E. et al. Atmospheric corrosion of bronze artefacts in museum indoor environments, EUROCORR 2019. In: *Proceedings of the European Corrosion Congress*, 9-13 September 2019, Seville, Spain, **2019**, (on electronic media, unpaged).
12. Lane H. The conservation and storage of lead coins in the department of coins and medals, *Recent Advances in Conservation and Analysis of Artefacts*, **1987**, 149–153.
13. Tétreault J. et al. Corrosion of copper and lead by formaldehyde, formic and acetic acids vapours, *Studies in Conservation*, **2003**, 48, 237–250.
14. Pecenova Z., Kouril M. Protection of historical lead against acetic acid vapour, K*OM – Corrosion and Material Protection Journal*, **2016**, 60 (1), 28–34.
15. Prosek T. et al. Real-time monitoring of indoor air corrosivity in cultural heritage institutions with metallic electrical resistance sensors, *Studies in Conservation*, **2013**, 58, 117–128.
16. Oesch S., Faller M. Environmental effects on materials: The effect of the air pollutants SO_2, NO_2, NO and O_3 on the corrosion of copper, zinc and aluminium. A short literature survey and results of laboratory exposures, *Corrosion Science*, **1997,** 39(9), 1505–1530.
17. Strandberg H. et al. The Atmospheric corrosion of statue bronzes exposed to SO_2 and NO_2. *Materials and Corrosion/ Werkstoffe und Korrosion*, **1997,** 48 (11) 721–730.
18. Lindström R. The Atmospheric Corrosion of Zinc in the Presence of NaCl. *Journal of Electrochemical Society*, **2000,** 147 (1751).
19. García-Segura A. et al. Influence of gaseous pollutants and their synergistic effects on the aging of reflector materials for concentrating solar thermal technologies. *Solar Energy Materials and Solar Cells*, **2019,** 200, 2–17.
20. Vera R. et al. Effect of atmospheric pollutants on the corrosion of high power electrical conductors: Part 1. Aluminium and AA6201 alloy. *Corrosion Science*, **2006**, 48 (10) p. 2882–2900.
21. Qafsaoui W. et al. Corrosion protection of bronze using 2,5dimercapto1,3,4thiadiazole as organic inhibitor: spectroscopic and electrochemical investigations, *Journal of Applied Electrochemistry,* **2019**, 49, 823–837.
22. Ingo G. M. et al. Surface studies of patinas and metallurgical features of uncommon high-tin bronze artefacts from the Italic necropolises of ancient Abruzzo (Central Italy), *Applied Surface Science*. **2019**, 470, 74-83.
23. Fabrizi L. et al. The application of non-destructive techniques for the study of Corrosion patinas of ten Roman silver coins: The case of the medieval Grosso Romanino, *Microchemical Journal,* **2019**, 145, 419-427.
24. ISO 8407:2009. Corrosion of metals and alloys – Removal of corrosion products from corrosion test specimens, **2009**.
25. Selwyn L. et al. Lead (Pb), In: *Metals and Corrosion: A Handbook for the Conservation Professional*. 1st ed., Canadian Conservation Institute: Canada, **2004**, 115-123. ISBN 0-662-37984-5.
26. Costa V., Urban F. Lead and its alloys: metallurgy, deterioration and conservation, *Reviews in Conservation,* **2005**, 6, 42-68.

27. Brimblecombe P. The composition of museum atmospheres, *Atmospheric Environment*, **1990**, 24B, 1-8.
28. Kouřil M. et al. Lead Corrosion and Corrosivity Classification in Archives, Museums, and Churches, *Materials,* **2022**, 15 (2), 639.
29. Švadlena J. et al. Protective ability of lead corrosion products in indoor atmosphere with acetic acid vapours, *KOM – Corrosion and Material Protection Journal,* **2021,** 65 (4), 1-6.
30. Strachotová K. et al. High-sensitivity sensors for monitoring of lead atmospheric corrosion, In: *Proceedings 30th Anniversary International Conference on Metallurgy and Materials*, METAL 2021, 26-28 May 2021, Brno, Czech Republic, **2021**, 639-941. ISBN: 978-80-87294-99-4
31. Majtás D., Fialová P. Optical evaluation of corrosion products using colorimetric spectroscopy, *In: Proceedings 28th International Conference on Metallurgy and Materials* METAL 2019, 22-24 May 2019, Brno, Czech Republic. **2019**, 1607-1614. ISBN: 978-80-87294-92-5
32. Majtás D. et al. Failure of electric products by H_2S, *KOM – Corrosion and Material Protection Journal*, 62 (2), **2018**, 71–77.
33. Watt J. et al. (Eds.) *The Effects of Air Pollution on Cultural Heritage,* **2009**, ISBN: 978-0-387-84892-1